ACS APPLIED MATERIALS & INTERFACES

Letter

www.acsami.org

Anti-icing Coating with an Aqueous Lubricating Layer

Renmei Dou,[†,‡] Jing Chen,[†] Yifan Zhang,[†,‡] Xupeng Wang,[†] Dapeng Cui,[†] Yanlin Song,[†] Lei Jiang,[†] and Jianjun Wang*[,†]

[†]Institute of Chemistry, Chinese Academy of Sciences, Beijing 100190, P. R. China

[‡]Graduated University of Chinese Academy of Sciences, Beijing 100049, P. R. China

Supporting Information

ABSTRACT: In this paper, an anti-icing coating with an aqueous lubricating layer is reported. This anti-icing coating can be directly applied to various substrates, and the ice adhesion strength on the coated surfaces can be lowered greatly as compared to uncoated substrates. We demonstrate for the first time that the formed ice on this anti-icing coating can be blown off by a wind action in the wind tunnel with a controlled temperature and wind velocity. Moreover, the low ice adhesion of the anti-icing coating can be maintained even when the temperature is lowered to -53 °C. The robustness and durability of the anti-icing coating are proved by the icing/de-icing experiments. The results show that the anti-icing coating with an aqueous lubricating layer is of great promise for practical applications.

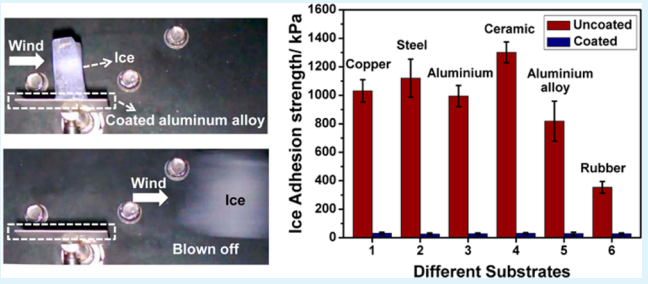

KEYWORDS: *aqueous lubricating layer, anti-icing coating, hydrophilic component, robustness and durability, low ice adhesion*

INTRODUCTION

Ice accumulation on various surfaces causes serious problems in our daily life. In some cases, it causes disastrous events such as crash of aircrafts and collapse of power networks, which result in severe economic impacts and large loss of lives.[1−3] Over the past decades, scientists have focused on superhydrophobic surfaces for delaying or preventing ice formation.[4−13] However, the superhydrophobicity would be lost in high humidity or be destroyed under the de-icing process, and the ice adhesion strength would be enlarged when ice penetrates into the surface texture.[10−18] Recently, a film of lubricating oil locked in micro/nanoporous substrates for anti-icing has been reported.[19−22] The lubricating oil film reduces the ice adhesion dramatically, which enables the easy removal of the accumulated ice.[19−21,23] It would be better if it had long-term durability by preventing the depletion of the oil via evaporation or wicking away by the formed ice.[24−26] In our previous work, we have developed a prototype anti-icing coating with cross-linked hygroscopic polymers grafted inside photolithographically prepared micropores on a silicon wafer surface.[27] This method reduces the ice adhesion strength greatly, and does not have problem of durability because water can be resupplied from moisture or melted ice. However, this prototype coating is of limited usage, because it is not practical to prepare micropores and to graft cross-linked hygroscopic polymers in the micropores on different types of solid substrates. Thus, it is more desirable to have a mechanical robust coating with a durable lubricating aqueous layer, and most importantly the coating can be applied directly on varieties of solid surfaces. The latter point is crucial for practical applications of anti-icing coatings.

Herein, we report a directly applicable, robust, and durable anti-icing coating with an aqueous lubricating layer. Polymers with hydrophilic pendant groups were synthesized, the introduced hydrophilic component can absorb water in humid environments and the pendant groups ionize in the water. Or it melts the ice or snow and swells once the particles are in contact with the ice or snow because ions in the solution lowers the water activity.[28] Thus, an aqueous lubricating layer forms on the coating even at subzero environments. It forms when icing occurs and remains as long as ice stays atop, which ensures the durability of the lubricating layer for the anti-icing application. We demonstrate for the first time that the formed ice on this anti-icing coating can be blown off by a wind action in the wind tunnel with a controlled temperature and wind velocity, because the ice adhesion strength on this coating is reduced greatly. Most importantly the coating can be directly applied to solid surfaces such as metals, metal alloys, ceramics and polymers. The existence of the aqueous lubricating layer is shown to be as low as −53 °C. Meanwhile, the robustness and durability of the coating are confirmed by the icing/de-icing experiment.

RESULTS AND DISCUSSION

We choose polyurethane as the main component for the anti-icing coating because it adheres firmly with varieties of solid surfaces.[29,30] Hydrophilic component dimethylolpropionic acid

Received: March 1, 2014
Accepted: May 14, 2014
Published: May 14, 2014

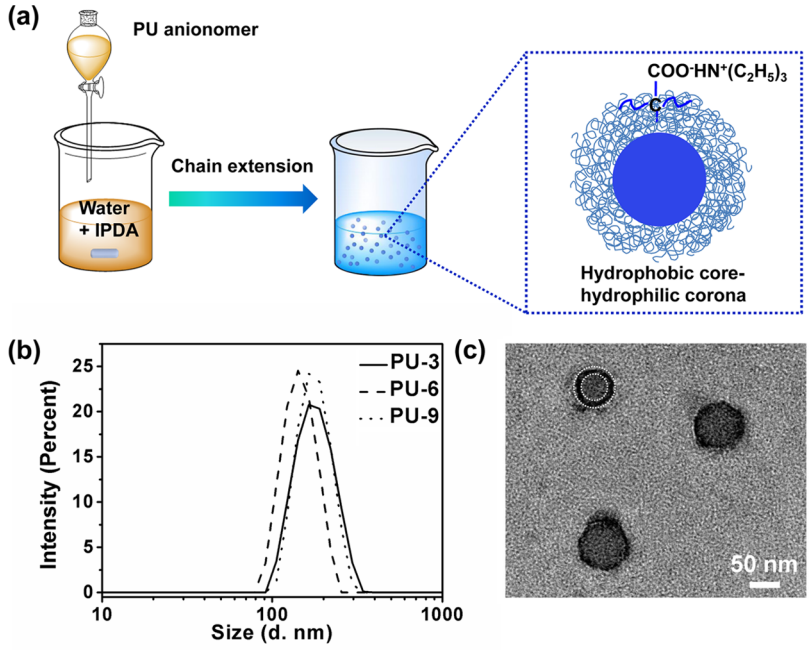

Figure 1. (a) Preparation of the core−corona particles dispersion. (b) Size of the hydrophobic core-hydrophilic corona particles characterized by the DLS. The solid line, dash line, and dot line represent PU-3, PU-6, PU-9, respectively. (c) Typical TEM image of the hydrophobic core−hydrophilic corona particles (PU-6). The particles were stained by phosphotungstic acid, and the dark corona is due to the preferential staining of the exterior hydrophilic component, which confirms the successful formation of the hydrophobic core−hydrophilic corona structure.

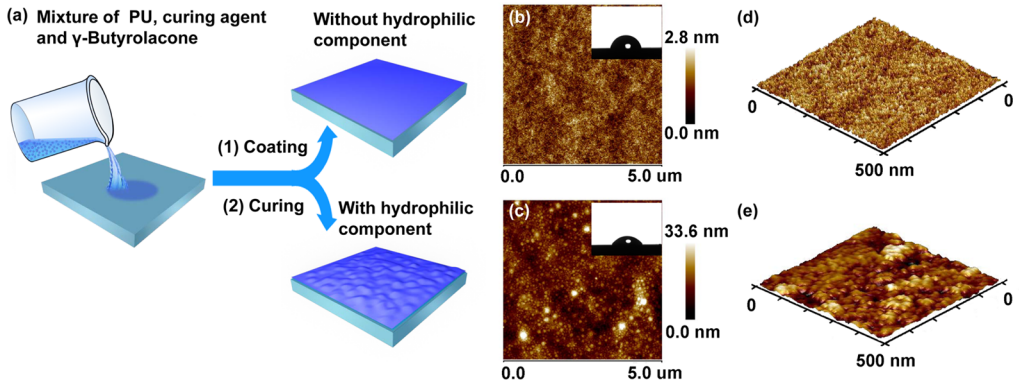

Figure 2. (a) Schematic illustration of the preparation of the anti-icing coating. The mixtures of PU, curing agent and γ-butyrolacone were spin-coated on the substrate, and then thermally cured to form a coating. The top and bottom images are the coating of PU with and without the hydrophilic component, respectively. (b, c) Morphology of the PU coating without and with the hydrophilic component characterized by AFM (The image size is 5 μm × 5μm). There are no spherical particles on the coating consisting of PU-0 without hydrophilic component in b. In contrast, spherical particles can be found on the surfaces of PU coatings with hydrophilic DMPA component as presented in c, and the diameters of these particles are consistent with the size observed in the TEM image. The insets represent the CAs of the coatings (98 and 43°). (d, e) 3D images of the PU coating without and with the hydrophilic component (image size is 500 nm × 500 nm). The PU coating with hydrophilic component is rougher, and the bump can be seen obviously because of the existence of the spherical particles.

(DMPA) component is covalently introduced into the polymer chain as shown in Figure S1 in the Supporting Information, and the PU dispersion was prepared. Figure 1a schematically illustrates the preparation of PU dispersion. The polyurethane anionomer was quickly added into water and chain-extended by reacting with isophorone diamine (IPDA). Because liquid water is used as a reaction medium, and the polymer chain consists of hydrophobic and hydrophilic components, the polymer chain entangles and forms spherical particles. The hydrophilic hard component migrates to the exterior of the particle forming hydrophilic corona, and the hydrophobic one stays in the interior forming hydrophobic core.[31]

Four kinds of PUs with different weight content of the hydrophilic component (DMPA) were synthesized and investigated for their anti-icing performance. PU-0, PU-3, PU-6, PU-9 represent the weight content of DMPA at 0, 3.0, 6.0, and 9.0 wt % in the polymer particles, respectively. Infrared spectroscopy (IR), X-ray diffraction (XRD) (see Figure S2 in the Supporting Information), and ^{1}H-NMR spectrum (see Figure S3 in the Supporting Information) were used to characterize the polymers. The molecular weight of the polymers was obtained by Gel Permeation Chromatography (GPC) (see Table S1 in the Supporting Information) Each XRD line exhibits a broad diffraction halo at $2\theta = 19°$ which is a fingerprint peak of PU.[32,33] In the IR spectra, the peak at 1600

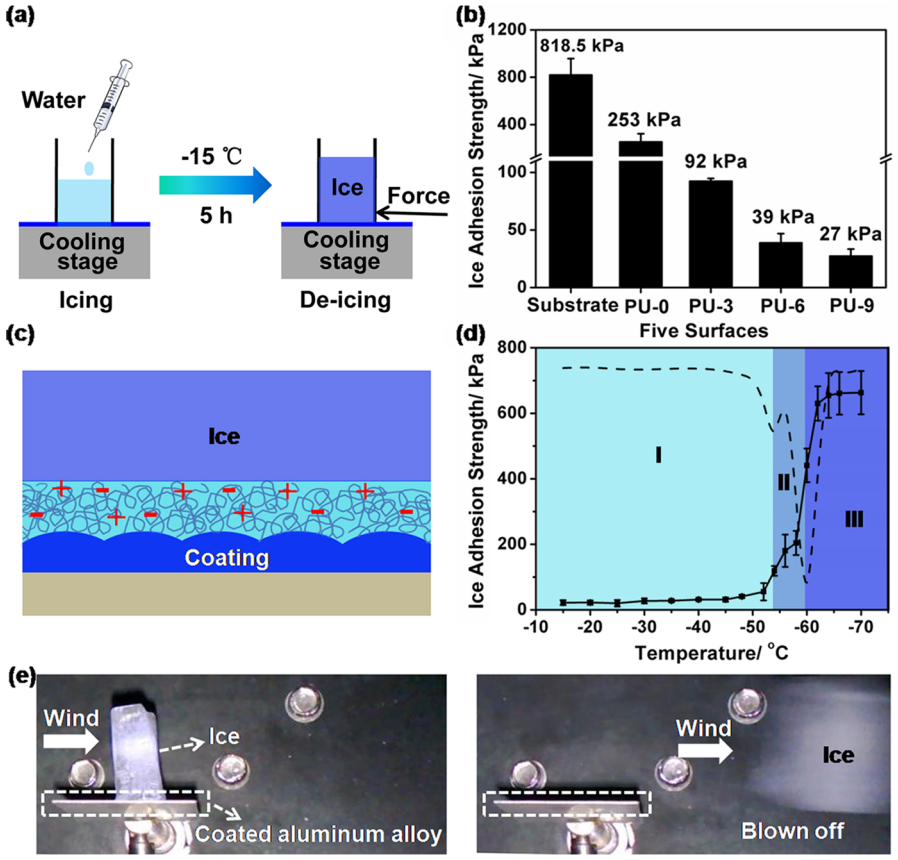

Figure 3. (a) Schematic depiction of the procedure used to test the ice adhesion strength. The bottomless cuvettes in close contact with the coated surfaces were filled with liquid water (Milli-Q), and the ice adhesion was tested after they were kept at −15 °C for 5 h to ensure the complete freeze of liquid water. (b) Ice adhesion strength on PU coatings with different weight content of the hydrophilic component. The ice adhesion strength on the uncoated aluminum alloy surface is around 800 kPa. As the anti-icing coating was spin-coated on the substrates, the ice adhesion strength reduced greatly. (c) The mechanism for the reduction of the ice adhesion by the introduction of an aqueous lubricating layer. (d) Ice adhesion strength of PU-9 at different temperatures. The solid line is the ice adhesion strength, and the dash line is differentiated from the solid line. Regimes of I−III represent the aqueous lubricating layer disappeared with the decreasing of the temperature. (e) Effectiveness of the anti-icing coating with an aqueous lubricating layer was tested in the wind tunnel. The ice on the anti-icing could be blown off with a strong breeze. Arrows denote direction of the wind.

cm^{-1} is attributed to the carboxylate $-COO^-$ stretching vibration, and the peak at 1730 cm^{-1} is attributed to the −C═O stretching vibration, and the differences in the peak intensity confirm the successful introduction of the hydrophilic component in PU with various content.[33−36]

Dynamic light scattering (DLS) and transmission electron microscope (TEM) were used to investigate the core−corona structure of latex particles and their sizes. The hydrodynamic radii of the particles were characterized by DLS in Figure 1b, which showed that diameters of the PU particles are almost the same, and the particle size distributions were presented in Figure S4 in the Supporting Information. Here PU-6 was chosen to characterize the microstructure of PU latex particles. In the TEM characterization, the PU latex particles were stained by phosphotungstic acid. Figure 1c is a typical TEM image of the PU-6 latex particle, and it clearly shows a concentric layered structure, and the exterior of the particle is black because of the exterior hydrophilic component is stained (Figure 1c).[31] This confirms that the hydrophilic hard components migrated to the exterior of the particle and formed a core−corona structure in the dispersion during the chain extension. It can be seen from the TEM image, the diameter of the particles is 69 ± 2 nm. In contrast, the hydrodynamic diameter of PU-6 particles dispersed in water is much larger than the size observed in TEM image. The increase of the particle size when dispersed in water indeed verifies the particles swell substantially, as illustrated in the right side of Figure 1a.

As shown in Figure 2a, PU coatings with and without the hydrophilic components were prepared. The morphology of the coatings was investigated by atomic force microscope (AFM) shown in Figure 2b−e. Images b and c in Figure 2 represent the AFM images of the PU-0 and PU-6 coatings, respectively, and the insets are the water CAs of the PU coatings. Figure 2b shows there are no spherical particles on the coating consisting of PU-0. In contrast, spherical particles can be found on the surfaces of PU-6 coatings with hydrophilic component as presented in Figure 2c, and the diameters of these particles are consistent with the size observed in the TEM image. In the 3D images (Figure 2d, e), the morphology of the coatings can be seen more obviously, the PU-6 coating with hydrophilic component is rougher than the PU-0 coating due to the existence of the spherical particles. The more hydrophilic component was introduced, the more hydrophilic of the PU coating is (see Figure S5 in the Supporting Information).

The ice adhesion strength was tested by a home-built apparatus which consists of a cooling stage, force transducer as depicted in Figure 3a. The results of ice adhesion strength on

dx.doi.org/10.1021/am501252u | ACS Appl. Mater. Interfaces 2014, 6, 6998−7003

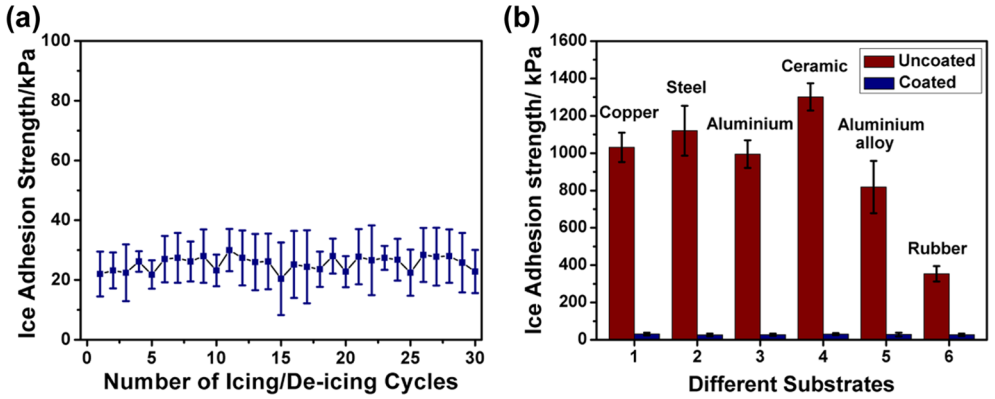

Figure 4. Robustness, durability, and applicability of the anti-icing coating. (a) Variation of the ice adhesion strength on the PU-9 coated sample with the number of icing/de-icing cycles, and it can be seen that the ice adhesion remains almost the same after the icing/de-icing test, which proves the robustness and durability of the coating. (b) Ice adhesion strength on different substrates before and after spin-coated with the anti-icing coating, which clearly shows that the coating is directly applicable on a wide range of substrates.

the PU coatings are presented in Figure 3b. The ice adhesion strength on the uncoated substrate (aluminum alloy 6061) is around 800 kPa. When the PU-0 film was coated on the substrate, the ice adhesion strength reduced to 200.5 ± 69.3 kPa. The ice adhesion strength on the PU-0 coating is consistent with the value reported by Murase and Laforte.[37,38] The reduction of the ice adhesion can be ascribed to two effects: (1) the PU coating reduces the roughness of the aluminum alloy surface, thus the mechanical interlocking between the ice and the surface texture is minimized;[11] (2) there is bound water around amide group and the freezing point of this water is greatly lower than that of bulk water.[39] The bound water is different from the free water in the aqueous solution, it can only form a very thin lubricating layer of a few molecules thickness, which should be in the regime of a boundary lubrication due to the thickness of the lubricating layer is far smaller than the surface roughness.[40] When the hydrophilic component was introduced, the ice adhesion reduced pronouncedly. The average ice adhesion strength of PU-9 was 27.0 ± 6.2 kPa, which is close to the value measured on the pre-perfused oil lubricating surface.[19] The low value of ice adhesion can be attributed to existence of the aqueous lubricating layer between ice and the coating. The aqueous lubricating layer acts as the lubricant on the surface, and at the same time it eliminates the defects on the solid surface which could make the surface much smoother, thus preventing the mechanical interlocking as shown in Figure 3c. The difference of the ice adhesion strength on the coatings with different content of DMPA should be due to different amount of free water the coatings can hold. The more the content of DMPA of PU, the more free water it can hold and the thicker aqueous lubricating layer forms on the surface, and thus it might enter the mixed or even hydrodynamic lubrication regime and the ice adhesion strength can be reduced greatly.[40]

The existence of the aqueous lubricating layer was further verified by investigating the temperature dependence of the ice adhesion strength on the anti-icing coating. Figure 3d shows the variation of the ice adhesion strength with the temperature. The solid line is the ice adhesion strength of PU-9, the dash line is differentiated from the solid line. In the differential curve calculated from the solid line, two peaks can be found at −53 and −60 °C. These two peaks are the transition temperatures of the ice adhesion in the solid line. It can be seen from Figure 3d, there three stages: (I) The values maintained around 27 kPa without obvious changes from −15 to −53 °C; (II) ice adhesion strength increased rapidly up to 200 kPa at the range of −53 to −60 °C; (III) the value rose sharply afterwards and then saturates at 700 kPa. At −53 °C, the ice adhesion strength is almost 200 kPa, which is closed to that of PU-0. Thus, the first transition temperature can be attributed to the freezing of free water in the aqueous lubricating layer on PU coatings with the hydrophilic component. As illustrated in Figure 3c, the introduced hydrophilic component can absorb water in humid environments and the pendant groups ionize in the water. Or it melts the ice or snow and swells once the particles are in contact with the ice or snow because of the lowered water activity.[28] Thus, an aqueous lubricating layer forms on the coating consisting of these core−corona particles even at subzero environments. Due to the existence of the aqueous lubricating layer, the ice adhesion strength on this coating can reduce greatly. The second transition temperature around -60 °C might be the freezing of the bound water around amide groups.[39] The low ice adhesion strength values above −53 °C should be at the mixed or even hydrodynamic lubrication regime, and at −53 °C it enters the boundary lubrication regime. At −60 °C, the lubricating layer disappears completely.

In order to simulate real environments for the anti-icing effects of the coating, the aluminum alloy sheets with and without anti-icing coating (PU-9) were investigated in a wind tunnel with a controlled temperature, wind velocity, and water content (see Figure S4 in the Supporting Information).[41,42] The ice was blown with an action of wind, and the whole process was captured by a video camera. As presented in Figure 3e which was screenshot from the Movie SI (see the Supporting Information), ice adhered on the coating before the wind action. Under the wind action, the ice went with the wind of 12 m/s; according to the beaufort wind scale, this wind force is a strong breeze. However, ice adhered on the uncoated aluminum alloy too firmly to be blown off even under the wind at the rate of 30 m/s, which is the highest wind force of the wind tunnel. The huge difference between uncoated and coated aluminum alloy surfaces confirms the anti-icing coating with an aqueous lubricating layer have excellent performance on reducing the ice adhesion.

The robustness and durability are one of the most important properties of the anti-icing coating. Previous report showed that superhydrophobic surfaces could reduce the ice adhesion to less than 100 kPa, but it was enlarged to 200 kPa after the icing/de-

icing cycles.[12] To confirm the robustness and durability of our anti-icing coating, the ice adhesion strength of the PU-9 was tested for 30 icing/de-icing cycles. Figure 4a depicts the relationship between the ice adhesion strength of the PU-9 anti-icing coating and the icing/de-icing cycles. It can be seen from Figure 4a that the ice adhesion strength maintains at low value without obvious changes after 30 icing/de-icing cycles. This means the coating with an aqueous lubricating layer has great mechanical robustness and durability. It can be attributed to the following two reasons. First of all, the adhesion of the PU coating to the substrate is strong and it is not removed from the aluminum alloy surface during the icing/de-icing process. Second, the aqueous lubricating layer is a water stimulus lubricating layer, which can be formed once ice formed atop during the icing/de-icing process.

Direct applicability of this anti-icing coating on different substrates was also investigated, which is crucial for practical applications of the anti-icing coatings. Ice adhesion strength of PU-9 coated metals, metal alloys, ceramics, and polymer surfaces were tested. As depicted in Figure 4b, the ice adhesion strengths reduced substantially when PU-9 coated on different substrates. It demonstrates clearly that our anti-icing coating can be directly applied on different surfaces.

CONCLUSIONS

In this paper, an anti-icing coating with an aqueous lubricating layer was prepared, where the aqueous lubricating layer forms via absorption the water from the moisture or melted ice. This coating can be directly applied to various substrates such as metals, metal alloys, ceramics, polymers, the ice adhesion strength on coated surfaces can be lowered to 30.0 kPa. The ice formed atop can be blown off with an action of a strong breeze in a wind tunnel. The existence of the aqueous lubricating layer is verified to as low as -53 °C. The robustness and durability of the anti-icing coating were proved by the icing/de-icing experiments. All the experimental results showed that the anti-icing coating with aqueous lubricating layer is of great promise for practical applications.

ASSOCIATED CONTENT

Supporting Information

Experimental details, chemical structure of the polymer, XRD, IR characterization of PU, CAs of the PU films, and the schematic diagram of the wind tunnel. This material is available free of charge via the Internet at http://pubs.acs.org.

AUTHOR INFORMATION

Corresponding Author

*E-mail: wangj220@iccas.ac.cn.

Notes

The authors declare no competing financial interest.

ACKNOWLEDGMENTS

J.W. acknowledges sincerely the beneficial discussion with Prof. Dr. G. Wegner at Max-Planck Institute for Polymer Research. The authors thank Prof. Y. Chen from Chinese Academy of Meteorological Sciences for helping experiments in the wind tunnel. The authors are grateful for the financial support from the Chinese National Nature Science Foundation (Grants 51173196, 21121001), and the 973 Program (2012CB933801, 2013CB933004).

REFERENCES

(1) Meuler, A. J.; Smith, J. D.; Varanasi, K. K.; Mabry, J. M.; McKinley, G. H.; Cohen, R. E. Relationships between Water Wettability and Ice Adhesion. *ACS Appl. Mater. Interfaces* **2010**, *2*, 3100−3110.

(2) Farzaneh, M.; Ryerson, C. C. Anti-icing and Deicing Techniques. *Cold Reg. Sci. Technol.* **2011**, *65*, 1−4.

(3) Ryerson, C. C. Ice Protection of Offshore Platforms. *Cold Reg. Sci. Technol.* **2011**, *65*, 97−110.

(4) Guo, P.; Zheng, Y.; Wen, M.; Song, C.; Lin, Y.; Jiang, L. Icephobic/Anti-Icing Properties of Micro/Nanostructured Surfaces. *Adv. Mater.* **2012**, *24*, 2642−2648.

(5) He, M.; Zhang, Q.; Zeng, X.; Cui, D.; Chen, J.; Li, H.; Wang, J.; Song, Y. Hierarchical Porous Surface for Efficiently Controlling Microdroplets' Self-Removal. *Adv. Mater.* **2013**, *25*, 2291−2295.

(6) Zhang, Q.; He, M.; Chen, J.; Wang, J.; Song, Y.; Jiang, L. Anti-icing Surfaces Based on Enhanced Self-propelled Jumping of Condensed Water Microdroplets. *Chem. Commun.* **2013**, *49*, 4516−4518.

(7) Antonini, C.; Bernagozzi, I.; Jung, S.; Poulikakos, D.; Marengo, M. Water Drops Dancing on Ice: How Sublimation Leads to Drop Rebound. *Phys. Rev. Lett.* **2013**, *111*, 014501.

(8) He, M.; Wang, J.; Li, H.; Song, Y. Super-hydrophobic Surfaces to Condensed Micro-Droplets at Temperatures Below the Freezing Point Retard Ice/Frost Formation. *Soft Matter* **2011**, *7*, 3993−4000.

(9) Jonas, U.; Vamvakaki, M. From Fluidic Self-Assembly to Hierarchical Structures—Superhydrophobic Flexible Interfaces. *Angew. Chem., Int. Ed.* **2010**, *49*, 4542−4543.

(10) Meuler, A. J.; McKinley, G. H.; Cohen, R. E. Exploiting Topographical Texture to Impart Icephobicity. *ACS Nano* **2010**, *4*, 7048−7052.

(11) Chen, J.; Liu, J.; He, M.; Li, K.; Cui, D.; Zhang, Q.; Zeng, X.; Zhang, Y.; Wang, J.; Song, Y. Superhydrophobic Surfaces Cannot Reduce Ice Adhesion. *Appl. Phys. Lett.* **2012**, *101*, 111603.

(12) Kulinich, S. A.; Farhadi, S.; Nose, K.; Du, X. W. Superhydrophobic Surfaces: Are They Really Ice-Repellent? *Langmuir* **2011**, *27*, 25−29.

(13) Varanasi, K. K.; Deng, T.; Smith, J. D.; Hsu, M.; Bhate, N. Frost Formation and Ice Adhesion on Superhydrophobic Surfaces. *Appl. Phys. Lett.* **2010**, *97*, 234102.

(14) Fillion, R. M.; Riahi, A. R.; Edrisy, A. A Review of Icing Prevention in Photovoltaic Devices by Surface Engineering. *Renewable Sustainable Energy Rev.* **2014**, *32*, 797−809.

(15) Kulinich, S. A.; Farzaneh, M. How Wetting Hysteresis Influences Ice Adhesion Strength on Superhydrophobic Surfaces. *Langmuir* **2009**, *25*, 8854−8856.

(16) Kulinich, S. A.; Farzaneh, M. Ice Adhesion on Superhydrophobic Surfaces. *Appl. Surf. Sci.* **2009**, *255*, 8153−8157.

(17) Farhadi, S.; Farzaneh, M.; Kulinich, S. A. Anti-icing Performance of Superhydrophobic Surfaces. *Appl. Surf. Sci.* **2011**, *257*, 6264−6269.

(18) Wang, Y.; Xue, J.; Wang, Q.; Chen, Q.; Ding, J. Verification of Icephobic/Anti-icing Properties of a Superhydrophobic Surface. *ACS Appl. Mater. Interfaces* **2013**, *5*, 3370−3381.

(19) Kim, P.; Wong, T.-S.; Alvarenga, J.; Kreder, M. J.; Adorno-Martinez, W. E.; Aizenberg, J. Liquid-Infused Nanostructured Surfaces with Extreme Anti-Ice and Anti-Frost Performance. *ACS Nano* **2012**, *6*, 6569−6577.

(20) Vogel, N.; Belisle, R. A.; Hatton, B.; Wong, T.-S.; Aizenberg, J. Transparency and Damage Tolerance of Patternable Omniphobic Lubricated Surfaces Based on Inverse Colloidal Monolayers. *Nat. Commun.* **2013**, *4*, 2176.

(21) Wong, T.-S.; Kang, S. H.; Tang, S. K. Y.; Smythe, E. J.; Hatton, B. D.; Grinthal, A.; Aizenberg, J. Bioinspired Self-repairing Slippery Surfaces with Pressure-stable Omniphobicity. *Nature* **2011**, *477*, 443−447.

(22) Zhu, L.; Xue, J.; Wang, Y.; Chen, Q.; Ding, J.; Wang, Q. Icephobic Coatings Based on Silicon-Oil-Infused Polydimethylsiloxane. *ACS Appl. Mater. Interfaces* **2013**, *5*, 4053−4062.

(23) Anand, S.; Paxson, A. T.; Dhiman, R.; Smith, J. D.; Varanasi, K. K. Enhanced Condensation on Lubricant-Impregnated Nanotextured Surfaces. *ACS Nano* **2012**, *6*, 10122−10129.
(24) Rykaczewski, K.; Anand, S.; Subramanyam, S. B.; Varanasi, K. K. Mechanism of Frost Formation on Lubricant-Impregnated Surfaces. *Langmuir* **2013**, *29*, 5230−5238.
(25) Subramanyam, S. B.; Rykaczewski, K.; Varanasi, K. K. Ice Adhesion on Lubricant-Impregnated Textured Surfaces. *Langmuir* **2013**, *29*, 13414−13418.
(26) Nosonovsky, M. Materials Science: Slippery When Wetted. *Nature* **2011**, *477*, 412−413.
(27) Chen, J.; Dou, R.; Cui, D.; Zhang, Q.; Zhang, Y.; Xu, F.; Zhou, X.; Wang, J.; Song, Y.; Jiang, L. Robust Prototypical Anti-icing Coatings with a Self-lubricating Liquid Water Layer between Ice and Substrate. *ACS Appl. Mater. Interfaces* **2013**, *5*, 4026−4030.
(28) Koop, T.; Luo, B.; Tsias, A.; Peter, T. Water Activity as the Determinant for Homogeneous Ice Nucleation in Aqueous Solutions. *Nature* **2000**, *406*, 611−614.
(29) Chavarria, F.; Paul, D. R. Morphology and Properties of Thermoplastic Polyurethane Nanocomposites: Effect of Organoclay Structure. *Polymer* **2006**, *47*, 7760−7773.
(30) Chattopadhyay, D. K.; Raju, K. V. S. N. Structural Engineering of Polyurethane Coatings for High Performance Applications. *Prog. Polym. Sci.* **2007**, *32*, 352−418.
(31) Jiang, M.; Zheng, Z.; Ding, X.; Cheng, X.; Peng, Y. Convenient Synthesis of Novel Fluorinated Polyurethane Hybrid Latexes and Core−Shell Structures via Emulsion Polymerization Process with Self-emulsification of Polyurethane. *Colloid Polym. Sci.* **2007**, *285*, 1049−1054.
(32) Nanda, A. K.; Wicks, D. A.; Madbouly, S. A.; Otaigbe, J. U. Nanostructured Polyurethane/POSS Hybrid Aqueous Dispersions Prepared by Homogeneous Solution Polymerization. *Macromolecules* **2006**, *39*, 7037−7043.
(33) Lee, H.-T.; Lin, L.-H. Waterborne Polyurethane/Clay Nanocomposites: A Novel Effects of the Clay and Its Interlayer Ions on the Morphology and Physical and Electrical Properties. *Macromolecules* **2006**, *39*, 6133−6141.
(34) Coates, J. In *Encyclopedia of Analytical Chemistry*; Meyers. R. A., Ed.; John Wiley & Sons: Chichester, U.K., 2000; pp 10815−10837.
(35) Yoon Jang, J.; Kuk Jhon, Y.; Woo Cheong, I.; Hyun Kim, J. Effect of Process Variables on Molecular Weight and Mechanical Properties of Water-based Polyurethane Dispersion. *Colloids Surf., A* **2002**, *196*, 135−143.
(36) Pérez-Limiñana, M. A.; Arán-Aís, F.; Torró-Palau, A. M.; César Orgilés-Barceló, A.; Miguel Martín-Martínez, J. Characterization of Waterborne Polyurethane Adhesives Containing Different Amounts of Ionic Groups. *Int. J. Adhes. Adhes.* **2005**, *25*, 507−517.
(37) Murase, H.; Nanishi, K. On the Relationship of Thermodynamic and Physical Properties of Polymers with Ice Adhesion. *Ann. Glaciol.* **1985**, *6*, 146−149.
(38) Laforte, C.; Beisswenger, A. Icephobic Material Centrifuge Adhesion Test. In *Proceedings of the 11th International Workshop on Atmospheric Icing of Structures*; Montréal , 2005; pp 1−6.
(39) Ping, Z. H.; Nguyen, Q. T.; Chen, S. M.; Zhou, J. Q.; Ding, Y. D. States of Water in Different hydrophilic Polymers — DSC and FTIR Studies. *Polymer* **2001**, *42*, 8461−8467.
(40) Kietzig, A.-M.; Hatzikiriakos, S. G.; Englezos, P. Physics of Ice Friction. *J. Appl. Phys.* **2010**, *107*, 081101.
(41) Zheng, G.; List, R. Convective Heat Transfer of Rotating Spheres and Spheroids with Non-uniform Surface Temperatures. *Int. J. Heat Mass Transfer* **1996**, *39*, 1815−1826.
(42) List, R.; Lesins, G. B.; García-García, F.; McDonald, D. B. Pressurized Icing Tunnel for Graupel, Hail and Secondary Raindrop Production. *J. Atmos. Oceanic Technol.* **1987**, *4*, 454−463.